

\*\*TITLE\*\*  
*ASP Conference Series, Vol. \*\*VOLUME\*\*, \*\*PUBLICATION YEAR\*\**  
 \*\*EDITORS\*\*

## The outer ejecta of $\eta$ Carinae

Kerstin Weis

*Institut für Theoretische Astrophysik, Universität Heidelberg,  
 Tiergartenstr. 15, 69121 Heidelberg, Germany*

**Abstract.** The nebula around  $\eta$  Carinae consists of an inner bipolar structure, historically called the *Homunculus*, and the outer ejecta consisting mainly of a variety of knots of different sizes. They reach out to distances of up to  $30''$  or  $0.3$  pc from  $\eta$  Car. With high-resolution long-slit observations we mapped the outer nebula in order to analyze the global expansion pattern and to model the three dimensional structure of the ejecta. We find very different expansion velocities for the knots of the outer ejecta. In some cases they reach up to values as high as  $2000 \text{ km s}^{-1}$ . Typical expansion velocities lie at considerably lower values around  $400 - 600 \text{ km s}^{-1}$ , i.e., they are comparable to the expansion velocities found in the Homunculus. Remarkably, the expansion of the outer ejecta reveals a bidirectional motion pattern, which is consistent with the bipolar structure of the inner nebula. A general overview of the morphology and kinematics of the outer ejecta is given and put into context with the structure and kinematics of the inner part of the nebula, the Homunculus.

### 1. Introduction and historical background

$\eta$  Carinae has a bolometric luminosity of  $L = 10^{6.7} L_\odot$  which puts it among the most luminous stellar objects known (Humphreys & Davidson 1994; Davidson & Humphreys 1997). In the light of recent discussions about  $\eta$  Car being a binary (Damineli 1996; Damineli, Conti, & Lopes 1997; Stahl & Damineli 1998), it is noteworthy that the masses of the two components would still be between 65 and  $70 M_\odot$  each. Both components would therefore still be among the most massive stars. Historical records already show the variable behavior of  $\eta$  Carinae which was strongest during the star's giant eruption around 1843. At that time  $\eta$  Car reached  $-1^m$ , making it the second brightest star in the southern hemisphere at that time. After that event the visual luminosity declined steadily down to  $8^m$  within a few years. Starting around 1950 the brightness increased again and still does so today (for lightcurves see van Genderen & Thé 1984; Viotti 1995; Humphreys, Davidson, & Smith 1999 and references therein). During the eruption of 1843 at least parts, if not all, of the nebula around  $\eta$  Car formed. The nebula was not found until in 1938 van den Bos measured several components of the ‘ $\eta$  Argus system’ and noted that these ‘companions may be nebular nuclei’. Only years later Gaviola (1946; 1950) and Thackeray (1949; 1950) detected independently a nebulosity around  $\eta$  Carinae. Due to its odd and ‘little man-like’

shape, Gaviola named the nebula the *Homunculus*. Gaviola and Thackeray speculated already about a fuzzy and faint outer nebula or oval shell. With deeper images Walborn (1976) showed that the nebula around  $\eta$  Carinae was indeed much larger and consisted not only of the inner Homunculus. He identified several knots outside this structure and named them according to their positions and morphology. Examples are the *S ridge* and the *E condensations*. Ten years later, in 1985, using a *shift and add* method an image of the Homunculus was made adding up 200 short (0.25s) exposures. This image showed for the first time the bipolar nature of the Homunculus (Duschl et al. 1995): two lobes, one tilted towards the north-west, the other to the south-east. The lobes are separated by an equatorial disk, which is defined through the so-called *streamers*. With the launch of the *Hubble Space Telescope* (HST) the imaging capabilities improved even further and the first high-resolution image of the nebula around  $\eta$  Carinae of the HST supported the model of a bipolar Homunculus. Fig. 1 shows an  $H_{\alpha}$  (F656N-filter) HST image of the Homunculus and the outer structures. Note that the F656N filter does not only detect  $H_{\alpha}$  emission but also [N II] emission, since parts of the nebula show a large Doppler shift (see section 4.). In the following we will call only the inner bipolar structure the Homunculus, all features and knots outside do form the *outer ejecta*, including the structures defined by Walborn (1976).

Already Gaviola recognized a motion within the nebula comparing his images with older images in which individual parts of the nebula were recorded as additional stellar components. Identifying these components with brighter parts of the Homunculus he obtained an expansion of several arcseconds per century or about  $550 \text{ km s}^{-1}$ . A first detailed analysis of the expansion of the knots was compiled in Ringuelet (1958) and Gratton (1963). Here the measured expansion velocities again reach values of about  $500 \text{ km s}^{-1}$  if corrected for the distance, which is today believed to be around 2.3 kpc (Davidson & Humphreys 1997; Walborn 1995 and references therein). Using a longer time baseline (10 – 15 years) Walborn (1976), Walborn, Blanco, & Thackeray (1978), and Walborn & Blanco (1988) determined proper motions of the outer knots that range between  $280 \text{ km s}^{-1}$  and  $1360 \text{ km s}^{-1}$ . Modern measurements of the proper motion of the Homunculus are based on high-resolution HST images (Currie et al. 1996; Currie & Dowling 1999; Currie these proceedings). The velocities derived with this method range between  $10 - 1000 \text{ km s}^{-1}$ . An attempt to use old scanned images and resolution-degraded HST images was made by Smith & Gehrz (1998).

One of the earliest observations to obtain radial velocities from the Homunculus dates back to Thackeray (1961) who measured velocities  $\sim 850 \text{ km s}^{-1}$  for the permitted lines and  $220 \text{ km s}^{-1}$  for the forbidden lines. Assuming that the permitted lines show a Doppler shifted plus a scattered component he concluded that the expansion velocity of the Homunculus should be about  $630 \text{ km s}^{-1}$ . Newer long-slit spectra support these measurements. An extensive study of the radial velocity of the Homunculus and the outer ejecta was carried out by Meaburn (1994) and Meaburn et al. (1993; 1996 and references therein). The radial velocities derived reach from  $250 \text{ km s}^{-1}$  to at least  $-1200 \text{ km s}^{-1}$ . Fabry-Perot observations by Walborn et al. (1991) yield similar results.

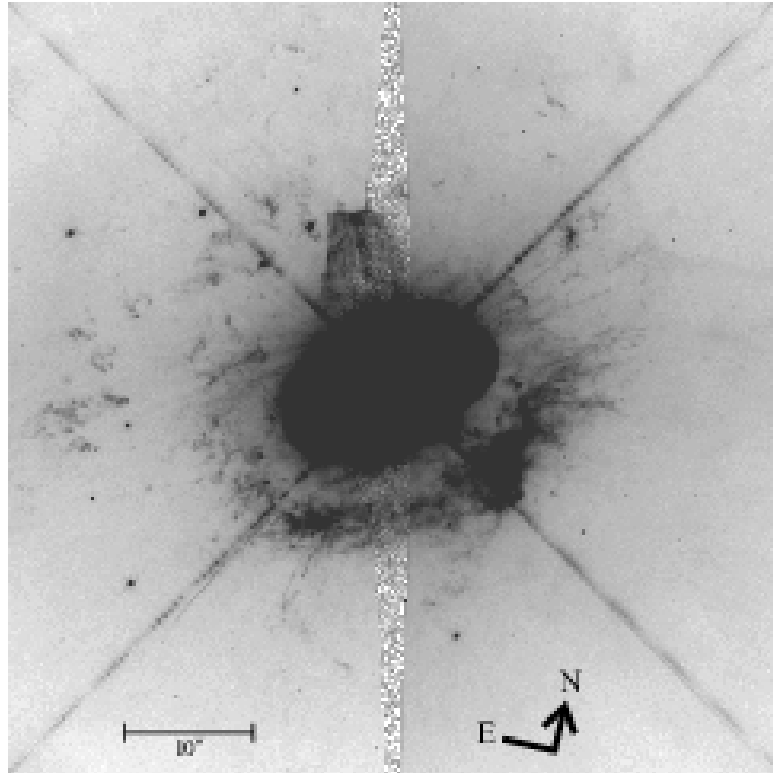


Figure 1. This figure shows a deep HST image in the F656N filter, about  $60'' \times 60''$  large. The contrast was optimized to emphasize especially the faint emission of the outer ejecta. The inner bipolar Homunculus appears as a more oval looking saturated structure in the center.

## 2. The new dataset and observations

In order to analyze the morphology and kinematics of especially the outer ejecta around  $\eta$  Carinae we obtained high-resolution long-slit echelle spectra with the 4 m telescope at the Cerro Tololo Interamerican Observatory. For order selection a post-slit  $H_{\alpha}$  filter was used and the cross disperser was replaced by a flat mirror. With the 79 l/mm grating the spectral resolution was about  $14 \text{ km s}^{-1}$  at the  $H_{\alpha}$  line. The slit length was vignetted to 4', the relevant section was only 1'.5. The pixel size in the spatial direction was  $0''.264$  per pixel. The observations were performed at a position angle (PA) of  $132^\circ$ , i.e., parallel to the major axis of the Homunculus. Starting at an offset star (star #60 in Thé, Bakker, & Antalova 1980) the spectra were offset  $2''$  to the north or south. *Slit 12S* is therefore a slit, offset by  $12''$  to the south of the offset star. The positions of all slits are depicted in Fig. 2. Note that due to the PA of  $132^\circ$  the  $2''$  offsets translate into a spacing between parallel slits of only  $1''.5$ . In all, 31 spectra were taken, of which the central 6 slits could not be used because of strong stray-light from the central star.

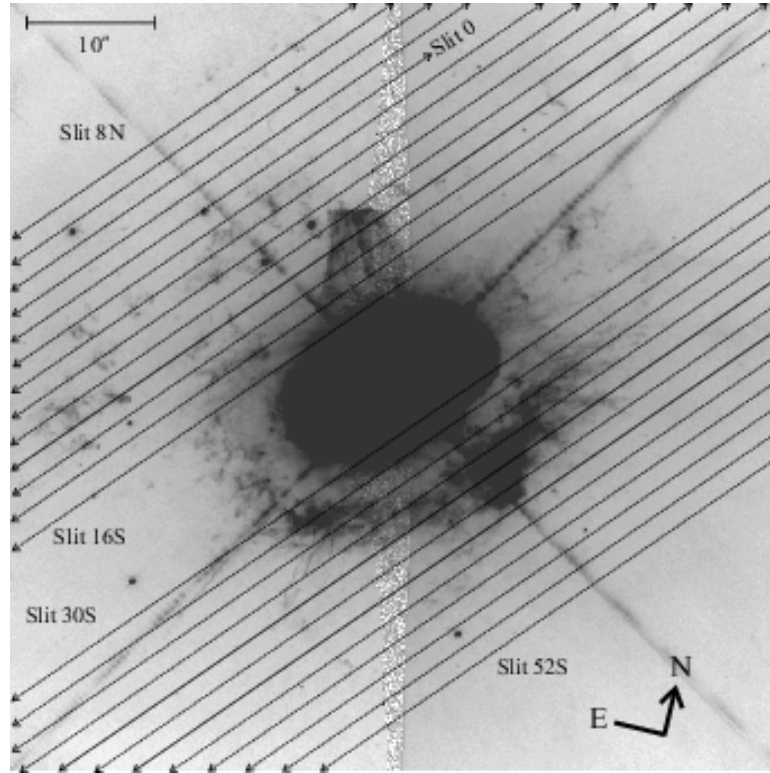


Figure 2. Here the same HST image as in figure 1 is shown, with our slit positions overplotted. The central 6 slit positions crossing the Homunculus are missing, since they could not be used due to strong stray-light. Solid lines indicate slits for which echellograms are depicted in figure 3.

### 3. The morphology of the outer ejecta

Using deep HST images taken with the F656N and F658N filter the outer ejecta was analyzed and its morphology studied. In contrast to the inner bipolar Homunculus the outer ejecta shows no clearly symmetric structure. A large amount of knots, bullets and filaments surround  $\eta$  Carinae up to a distance of 30" in radius (0.33 pc), compared to the inner Homunculus which has a diameter of 17" (about 0.2 pc). The sizes and shapes of the knots and filaments in the outer ejecta are manifold, reaching between 7"5 for the N condensation to fractions of arcseconds for the smallest structures. Most likely many small filaments are not resolved yet, and very faint, small structures are below the detection limit. The morphology of the structures in the outer ejecta represent those of irregular shaped knots and bullets, some might even be described as arches, some look more like long filaments. Most amazing are very straight, long collimated structures which in the following will be called *strings*, these structures are discussed in section 5. in more detail. Other than these individual structures the *South ridge* is the most remarkable feature in the outer ejecta. Here a large

amount of bullets seem to be connected or even more likely are running into each other. As it will be shown later these colliding knots are giving rise to X-ray emission from this area (see section 6. and Weis, Duschl, & Bomans 2000).

#### 4. The kinematics of the outer ejecta

The kinematics of the outer ejecta was studies using the high-resolution long-slit echelle data. For each knot detected in the spectra the minimum and maximum velocities were derived, as well as the velocity of its brightest emission. Fig. 3 shows 3 typical echellograms. Each one is 75 Å wide, centered on the  $H_{\alpha}$  line at rest, and a spatial section of 90'' is shown. In the echellogram red and blueshifted knots are visible and labeled by numbers. A single knot is a coherent structure, which may or may not consist out of several sub-entities visible due to their different intensities or velocities, see for example knot 7 in Slit 10S. Taking all measurements of the spectra together the following results were deduced:

- About 200 knots were identified from which the fastest redshifted feature moves with  $+2000 \text{ km s}^{-1}$  while the fastest blueshifted structures' velocity is  $-1200 \text{ km s}^{-1}$ .
- Most of the knots move slower but still with  $+600 \text{ km s}^{-1}$  to  $-600 \text{ km s}^{-1}$ . Note that these values are only lower limits of the true expansion velocities since we measure radial velocities, which do not take into account the projection angle. If it were  $45^{\circ}$  this would yield already velocities around  $850 \text{ km s}^{-1}$  for most of the knots.
- The largest spread in velocity of a single coherent knot was found to be  $1250 \text{ km s}^{-1}$ .

Beside these results for individual knots also a global trend of the expansion in the outer ejecta was discovered. Fig. 4 visualizes this result. In this figure the velocities of representative knots are overplotted onto an HST image. Blueshifted, negative velocities are underlined. A systematic distribution is then obvious: Knots with redshifted emission are concentrated towards the north-west of the star, while knots in the south-east show predominantly blueshifted lines. With respect to the central star, this represents a bidirectional motion pattern, i.e., also the outer ejecta shows a bipolar structure. If we compare the outer ejecta with the inner bipolar Homunculus, we can see a similarity. The north-western lobe of the Homunculus is tilted away from the observer, its net expansion is redshifted, while the south-eastern lobe is blueshifted, this lobe is tilted towards us. Therefore the Homunculus and the outer ejecta show not only both a bipolar morphology, but one with a very similar orientation.

In the echelle spectra also the  $[\text{N II}]\lambda 6583\text{\AA}/H_{\alpha}$  ratio could be measured, a rough indicator for the nitrogen overabundance of the ejecta. For knots in the outer ejecta  $[\text{N II}]\lambda 6583\text{\AA}/H_{\alpha}$  ratios between 1 and 5 were measured, with most of them around 3.

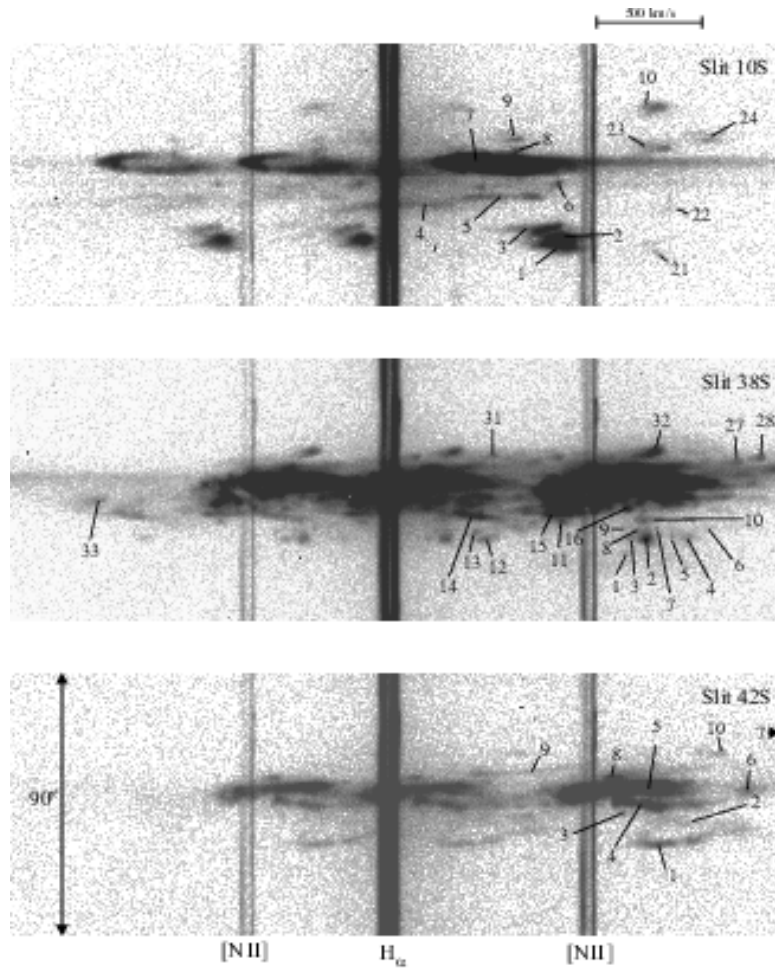


Figure 3. The 3 echellograms depicted here are  $75 \text{ \AA}$  wide and  $90''$  high. The positions of the slits are marked with solid lines in figure 2. On top of the echellograms a bar indicates a Doppler shift of  $500 \text{ km s}^{-1}$ .

## 5. Strings

In the outer ejecta, we found very straight, long and highly collimated structures the strings. They are of great interest in relation to the formation mechanism of the nebula around  $\eta$  Carinae. We identified 5 such strings in the nebula by visual inspection of the HST images. On much smaller scales numerous such structures can be found, but we do not count them among the strings since their collimation and parameters are not as extreme as those of the strings. With a length of 0.18 pc and a length-to-width ratio of 70 String 1 is the largest string and comparable in size to the entire Homunculus nebula. Images of the strings are shown in Fig. 5. In addition to their amazing morphological structure the strings show a strange kinematic behavior. Their radial velocity increases along the string outwards. Close to the star, String 1 moves with  $-522 \text{ km s}^{-1}$ , following the string outwards this velocity increases steadily up to  $\sim -1000 \text{ km s}^{-1}$  at the far

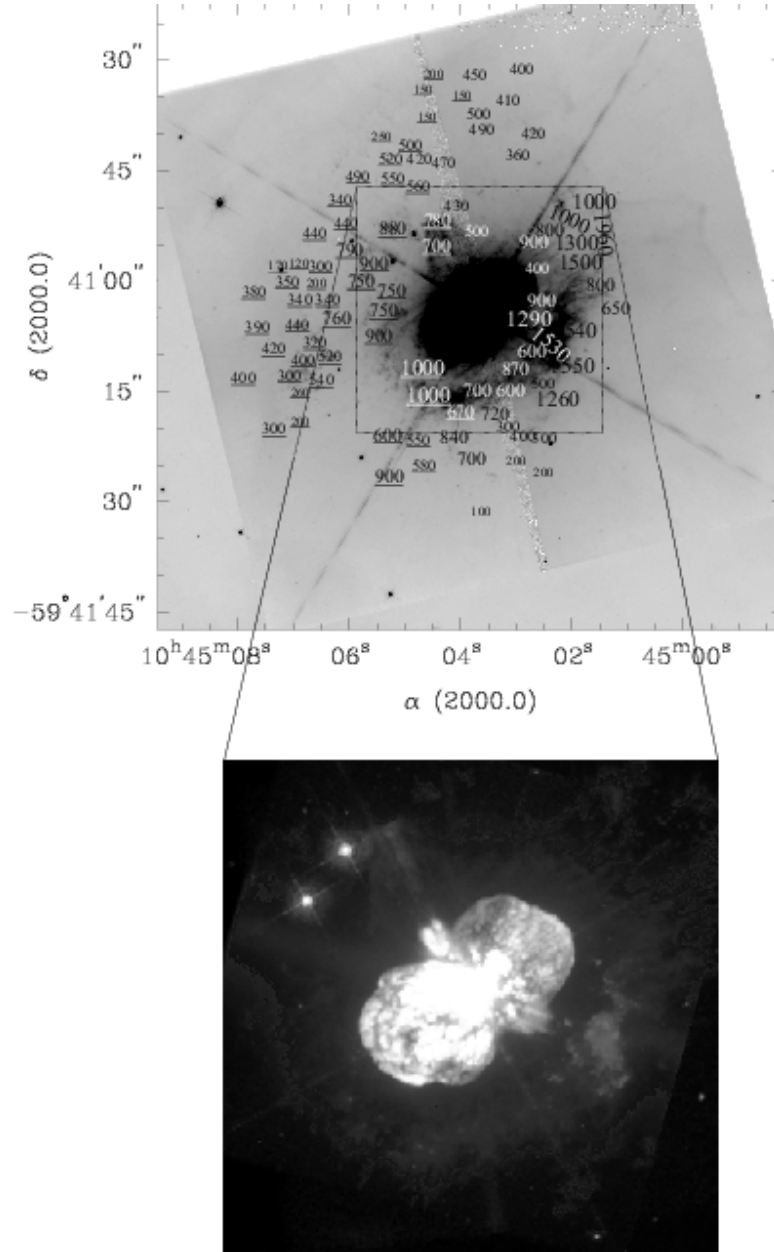


Figure 4. In the upper panel the same image as in Fig. 1 is shown. Onto the image, scaled by font sizes, the radial velocities of individual knots (with the highest velocity for a certain area) are overplotted. Underlined velocities represent negative (blueshifted) structures, not underlined ones are redshifted, positive values. A clear trend is visible, showing that blueshifted structures appear in the south-east while redshifted are concentrated to the north-west. The lower panel shows the central bipolar Homunculus for comparison.

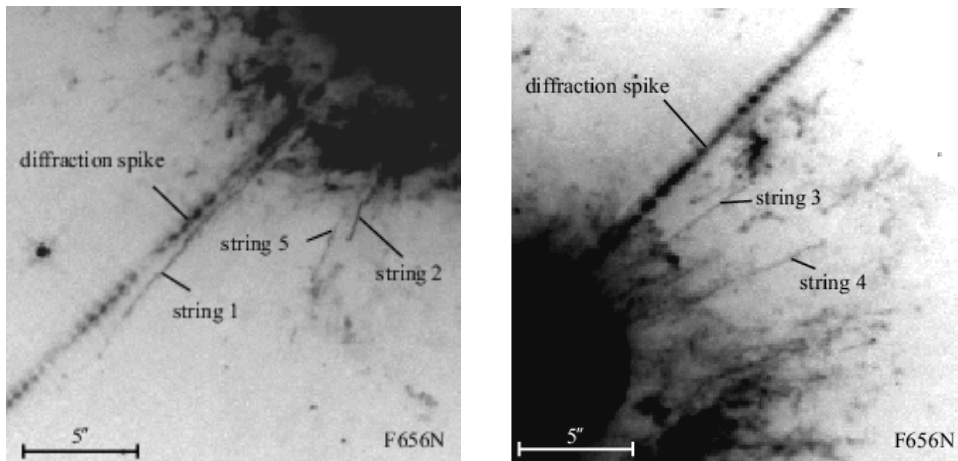


Figure 5. *Left:* Enlargement of the F656N HST image showing the strings 1, 2 and 5 in detail. *Right:* To the north-east of  $\eta$  Carinae, strings 3 and 4 are visible.

end. The strings follow an almost perfectly linear velocity law. Extrapolating the strings back to the star, this relation makes it exceedingly likely that the radial velocity reaches zero at the star. The strings show a Hubble type velocity law. A more detailed analysis of the strings can be found in Weis, Duschl, & Chu (1999). Still, it is not clear what the physical nature of the strings is. They may well be highly collimated coherent structures, similar to a water jet, for instance, but one may equally well envisage a train of many individual knots or bullets just following the same path. Another possibility is that they are trails or wakes following an object at the strings' far ends, or even projection effects of the walls of, for instance, much wider funnels. The origin and physics behind the strings is not solved yet. Recently, we have obtained HST-STIS data from which we expect to be able to conclude on their physical status (densities but also physical structure).

## 6. The X-ray emission from the outer ejecta

X-ray images of the nebula around  $\eta$  Carinae (Fig. 6., ROSAT HRI image overlaid as contours over an optical F656N filtered HST image) show no clear symmetry or coincidence with the optical emission. The X-ray emission is hook-shaped with two brighter maxima—one of which appears close to the S ridge. When comparing the X-ray emission not only with the optical emission but with the kinematics of the outer ejecta a much better correlation is found. X-rays are present where fast knots are located. The emission is due to fast knots producing shock waves. These shocks are presumably strongest where the density is highest. This is for instance in agreement with the bright X-ray spot being seen at the S condensation's location where many knots are indicative of higher density.

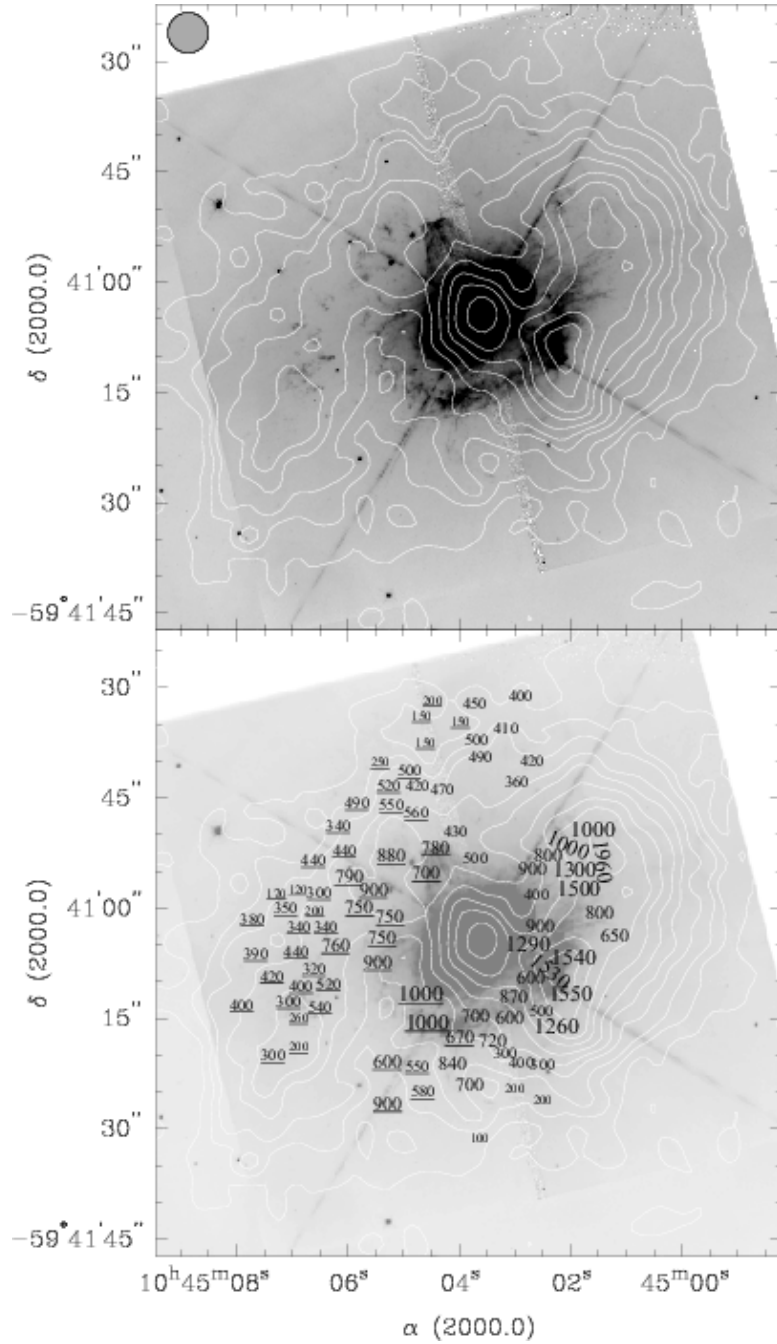


Figure 6. Overlay of the X-ray emission (contour lines) and an HST image (grey scales). The lower panel shows the same overlay as the upper panel (with decreased grey scale intensity), with the measured radial velocities (in  $\text{km s}^{-1}$ ) placed at their respective positions. Underlined numbers indicate negative velocities. The sizes of the characters increase with increasing absolute velocities (see text).

Since the majority of the knots in the outer ejecta shows velocities around  $400 \text{ km s}^{-1}$  to  $600 \text{ km s}^{-1}$  we derive a plasma temperature of  $2 - 5 \cdot 10^6 \text{ K}$ , using  $T_{\text{ps}} = V^2(3\mu/16k)$  (see McKee 1987;  $V$ : radial velocity taken as representative for the shock velocity;  $\mu$ : mean mass per particle). We assumed a normal He/H ratio of 0.1 leading to  $\mu = 0.61$  for a fully ionized gas. Since the material in the nebula around  $\eta$  Car contains a significant amount of CNO processed material the He/H ratio is most likely higher, which also increases the plasma temperature (by about a factor of 1.5 for He/H = 0.33). The highest X-ray emission results from two X-ray knots where the velocities measured from the spectra are much higher than average. Here the radial velocities ( $+1500$  and  $+1900 \text{ km s}^{-1}$ ) indicate equilibrium shock temperatures of  $3 \cdot 10^7$  and  $5 \cdot 10^7 \text{ K}$ . For further details of this analysis see Weis, Duschl, & Bomans (2000).

## 7. Summary and Conclusions

The outer ejecta is in many respects an outstanding nebula, which extends to about 0.33 pc in radius around  $\eta$  Carinae. The measured expansion velocities reach as high as  $2000 \text{ km s}^{-1}$ , i.e., much higher than expected and higher than detected earlier. The majority of the knots in the outer ejecta as well as the Homunculus itself move with velocities between  $+600$  and  $-600 \text{ km s}^{-1}$ . While the Homunculus shows a bipolar morphology, the knots in the outer ejecta seem randomly distributed and do not obviously follow a certain symmetry. However, taking the kinematic data into account, the outer ejecta *does* show a bipolar symmetry indicated by the distribution of blue and redshifted structures. The ejecta itself resembles a large collection of bullets of very different sizes and morphologies. Moving with higher velocities these knots form shocks which are then visible in X-rays. A comparison of the morphology of the X-ray emission with the kinematics of knots in the outer ejecta nicely demonstrates this coincidence.

**Acknowledgments.** Sincere thanks goes to Prof. Wolfgang J. Duschl for reading and improving the manuscript and to Dr. Dominik J. Bomans for inspiring discussions on the subject. This work was supported by the Deutsche Forschungsgesellschaft (DFG) through grant Du 168/8-1.

## References

Currie, D.G., Dowling, D.M., Shaya, E.J., et al. 1996, AJ, 112, 1115  
 Currie, D.G., Dowling, D.M. 1999, in *Eta Carinae at the Millennium*, ASP Conf. Ser., 179, eds.: Morse, J.A., Humphreys, R.M., Damineli, A., 72  
 Damineli, A. 1996, ApJ, 460, L49  
 Damineli, A., Conti, P.S., Lopes, D.F. 1997, New Astronomy, 2, 107  
 Davidson, K., Humphreys, R.M. 1997, ARA&A, 35, 1  
 Duschl, W.J., Hofmann, K.-H., Rigaut, F., Weigelt, G. 1995, RevMexAA SdC, 2, 17  
 Gaviola, E. 1946, Revista Astronomica, 18, 25  
 Gaviola, E. 1950, ApJ, 111, 408

Gratton, L., 1963, in *Star Evolution*, eds.: Gratton, L., New York Academic Press, 297

Humphreys, R.M., Davidson, K. 1994, PASP, 106, 1025

Humphreys, R.M., Davidson, K., Smith, N. 1999, PASP, 111, 1124

Meaburn, J., 1994, Ap&SS, 216, 241

Meaburn, J., Gehring, G., Walsh, J.R., et al., 1993, A&A, 276, L21

Meaburn, J., Boumis, P., Walsh, J.R., et al., 1996, MNRAS, 282, 1313

Ringuelet, A.E. 1958, Zeitschrift für Astrophysik, Vol. 46, 276

Smith, N., Gherz, R.D. 1998, AJ, 116, 823

Stahl O., Damineli A., 1998, in 'Cyclical Variability in stellar winds', proceedings of the ESO workshop, eds.: Kaper L., Fullerton A.W., Springer, 112

Thackeray, A.D. 1949, Observatory, 69, 31

Thackeray, A.D. 1950, MNRAS, 110, 524

Thackeray, A.D. 1961, Observatory, 81, 99

Thé P.S., Bakker R., Antalova A., 1980, A&AS, 41, 93

van den Bos, W.H. 1938, Union Observatory Circular, No. 100, 522

van Genderen, A.M., Thé, P.S. 1984, Space Sci.Rev., 39, 317

Viotti, R. 1995, RevMexAA SdC, 2, 10

Walborn, N.R. 1976, ApJ, 204, L17

Walborn, N.R., Evans, I.N., Fitzpatrick, E.L., Phillips, M.M., 1991, in IAU Symp., 143, *Wolf-Rayet Stars and Interrelations with Other Massive Stars in Galaxies*, eds.: van der Hucht, K.A., Hidayat, B., Kluwer, Dordrecht, Holland, 505

Walborn, N.R. 1995, RevMexAA SdC, 2, 51

Walborn, N.R., Blanco, B.M., Thackeray, A.D. 1978, ApJ, 219, 498

Walborn, N.R., Blanco, B.M. 1988, PASP, 100, 797

Weis, K., Duschl, W.J., Chu, Y.-H. 1999, A&A, 349, 467

Weis, K., Duschl, W.J., Bomans, D.J. 2000, A&A, submitted